EPJ Web of Conferences **140**, 09022 (2017) DOI: 10.1051/epjconf/201714009022
Powders & Grains 2017

A micromechanical approach of suffusion based on a length scale analysis of the grain detachment and grain transport processes

Antoine Wautier[1,2,3,⋆], *Stéphane* Bonelli[2], and *François* Nicot[3]

[1] *AgroParisTech-ENGREF, 19 avenue du Maine, 75732 Paris, France*
[2] *Irstea UR RECOVER, 3275 Rte Cézanne, CS 40061, 13182 Aix-en-Provence Cedex 5, France*
[3] *Université Grenoble Alpes, Irstea, UR ETGR, 2 rue de la Papeterie-BP 76, F-38402 St-Martin-d'Hères, France*

Abstract. Suffusion is the selective erosion of the finest particles of a soil subjected to an internal flow. Among the four types of internal erosion and piping identified today, suffusion is the least understood. Indeed, there is a lack of micromechanical approaches for identifying the critical microstructural parameters responsible for this process. Based on a discrete element modeling of non cohesive granular assemblies, specific micromechanical tools are developed in a unified framework to account for the two first steps of suffusion, namely the grain detachment and the grain transport processes. Thanks to the use of an enhanced force chain definition and autocorrelation functions the typical lengths scales associated with grain detachment are characterized. From the definition of transport paths based on a graph description of the pore space the typical lengths scales associated with grain transport are recovered. For a uniform grain size distribution, a separation of scales between these two processes exists for the finest particles of a soil

1 Introduction

Under various circumstances, fully saturated granular materials are subjected to internal flows which may modify their microstructure and consequently their overall hydraulic and mechanical properties. At the microscale, this process consists in a rearrangement of particles driven by three elementary mechanisms, namely the detachment of grains from the granular skeleton, their transport through the pore network and possibly their reattachment to the granular skeleton farther away. At a larger scale, this process results in the selective erosion of the smallest particles of a soil and is referred to as suffusion within the geomechanics community [1]. Despite many attempts to provide criteria to assess the suffusion susceptibility of a soil, the onset of the three cited elementary mechanism is still poorly understood.

With the recent development of fluid/grain coupling schemes and thanks to ever increasing computation power, it is now possible to address this issue from a micromechanical point of view. However, fully coupled three dimensional simulations of the suffusion of granular materials are still very demanding in terms of computation time and the number of particles which can be simulated in practice is limited.

In order to assess the ability of numerical simulations to be representative of the phenomenon at the microscale, this paper investigates the possibility of providing a quantitative definition of the length scales associated with the grain detachment and the grain transport mechanisms. First, the grain detachment mechanism is investigated thanks to the distinction between chained and non-chained particles [2] as the detachable particles should not be heavily stressed. Thanks to the computation of autocorrelation functions [3] a length scale associated with this mechanism is defined. Then, the grain transport mechanism is addressed with the description of the pore space in terms of a graph composed of pores and constrictions [4]. A propagation criterion is then introduced in order to define a length scale associated with this mechanism.

For the sake of illustration, these micromechanical tools are tested on a numerical sample composed of 10 000 spheres with radii uniformly distributed between $r_{\min} = 3.6 \times 10^{-5}$ m and $r_{\max} = 10\, r_{\min}$. A Discrete Element Method (DEM) is used in order to simulate the mechanical behavior of the individual grains and the simple elasto-frictional contact law introduced in [5]. This sample is first prepared in a dense configuration with a void index of 0.6 thanks to the radius expansion technique and is then subjected to a drained triaxial test up to 20 % of axial strain (denoted as ε_{zz}) and under a confining pressure of 100 kPa. This procedure enable the definition of a collection of microstructure configurations presenting the same global grading curve but exhibiting different grain arrangements subjected to various loading states.

2 Mesoscale analysis of the grain detachment mechanism

The microscale analysis of the grain detachment mechanism is underpinned by two governing ideas. First, the

⋆e-mail: antoine.wautier@irstea.fr

© The Authors, published by EDP Sciences. This is an open access article distributed under the terms of the Creative Commons Attribution License 4.0 (http://creativecommons.org/licenses/by/4.0/).

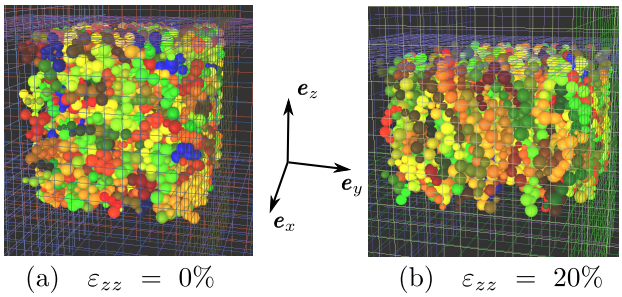

Figure 1. Force chains visualization under an isotropic confining pressure of 100 kPa (a) and at the end of the triaxial test (b).

most detachable grains should also be the least stressed in comparison with the local additional forces applied by the fluid. Then, the mesoscale associated with the grain detachment process should be linked to the inter-distance between the heavily stressed particles of the grain assembly. As a result, the solid fraction of a granular media can be divided into two groups of particles based on the force chain definition introduced in [2] according to the following three characteristics:

- Chained particles have a higher principal stress than the mean particle principal stress;
- Their principal stress direction is aligned with the geometrical contact direction (less than 45° deviation);
- Force chains are composed of at least three contacting particles.

A typical visualization of the force chains is visible in Figure 1 for the dense sample introduced in the Sect. 1 under an isotropic confining pressure of 100 kPa (Figure 1.a) and in the critical state at the end of the drained triaxial test (Figure 1.b). At the beginning of the triaxial test, the force chains are distributed in an isotropic way which is consistent with the fact that no principal direction of loading exists. Once the deviatoric loading is applied, the force chains tend to align in the vertical direction of the macroscopic principal stress. It should be also notice here that few particles belongs to the force chains as only 25 to 30 % of the total number of the particles composing the whole sample are visible in Figure 1. As the force chains align in the vertical direction to resist the deviatoric loading the number of chained particles also decreases by a sixth. The dual comment is that in the critical state, groups of loose particles bounded by force chains are larger than at the beginning of the triaxial test and that grain detachment is more likely to be observed in the critical state than in the initial state.

From the partition of the solid fraction of our sample between chained and non-chained grains a mesovolume is conceptually introduced to account for the grain detachment as a small box bounded by force chains and filled with non-chained grains. An estimate of the three dimensions of this mesovolume is then defined thanks to two-point spatial autocorrelation functions [3].

If Ω denotes the domain occupied by the chained particles of a given sample of volume V, the spatial autocorrelation

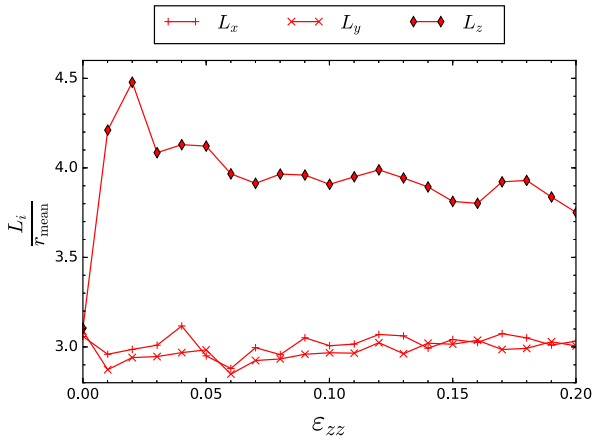

Figure 2. Strain evolution of the three autocorrelation lengths L_i ($i \in \{x, y, z\}$) during a drained triaxial test. The values are normalized by the grain mean radius r_{mean}.

function C is defined for any vector $\boldsymbol{h} = (h_x, h_y, h_z)$ as the joint probability that a point $\boldsymbol{x}$ and the translated point $\boldsymbol{x} + \boldsymbol{h}$ simultaneously belong to chained particles:

$$C : \begin{cases} \mathbb{R}^3 & \mapsto & \mathbb{R} \\ \boldsymbol{h} & \mapsto & \mathbb{P}\{\boldsymbol{x} \in \Omega \cap \boldsymbol{x} + \boldsymbol{h} \in \Omega, \forall \boldsymbol{x} \in V\} \end{cases} . \quad (1)$$

A dimensionless form of this function can be defined as $\tilde{C}(\boldsymbol{h}) = \dfrac{C(\boldsymbol{h}) - C(0)^2}{C(0) - C(0)^2}$. In this form, $\tilde{C}$ decreases from 1 to 0 as $\|\boldsymbol{h}\|$ goes from 0 towards $+\infty$, and the rate of decrease provide a typical distance over which the microstructure considered is correlated. Based on the integral range theory [3], the volume of the elementary box linked to the grain detachment mechanism is then defined by integrating $\tilde{C}$ over $\mathbb{R}^3$. With the use of an exponential fit as

$$\tilde{C}_{\text{fit}}(\boldsymbol{h}) = \exp\left(-2\pi^{1/3}\sqrt{\left(\frac{h_x}{L_x}\right)^2 + \left(\frac{h_y}{L_y}\right)^2 + \left(\frac{h_z}{L_z}\right)^2}\right) \quad (2)$$

the dimensions of the mesovolume associated with grain detachment are simply characterized by the three introduced length scales L_x, L_y and L_z.

In Figure 2, the strain evolution of these three autocorrelation lengths is plotted with respect to the axial strain ε_{zz} applied during the triaxial test introduced in Section 1.

As the horizontal autocorrelation lengths remains more or less constant around three times the grain mean radius r_{mean}, the vertical autocorrelation length increases up to a peak value of $4.5\, r_{\text{mean}}$ before decreasing and stabilizing around $4\, r_{\text{mean}}$ for $\varepsilon_{zz} > 15\%$. It is worth underlining here that these observations are closely related to the macroscopic mechanical response of the considered sample (not shown here) and is typical of a dense granular assembly. Indeed, the increase in the vertical autocorrelation corresponds to a lengthening of the force chains along this direction which accounts for the initial hardening of our dense sample. The following decrease in the vertical autocorrelation accounts for the destruction of force chains and thus for the stress softening regime observed classically for dense granular materials at large strain levels during triaxial tests.

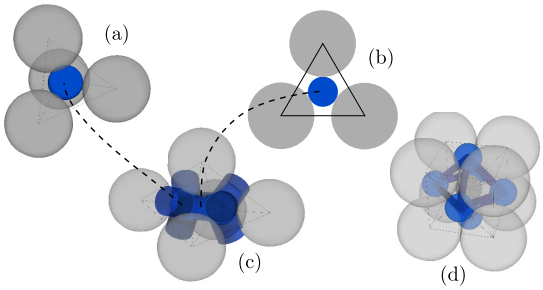

Figure 3. Visualization of different pore networks for an assembly of 5 grains (b) and 9 grains (d). Pores are represented as inscribed spheres (a) and constrictions as inscribed cylinders between pores (c).

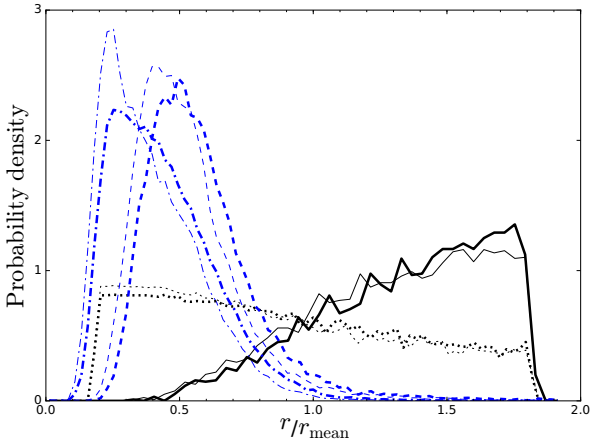

Figure 4. Probability densities for a constriction (dash-dotted line), a pore (dashed line), a chained grain (solid line) or a non-chained grain (dotted line) to be of a given radius. The thick line corresponds to $\varepsilon_{zz} = 20\%$, while the thin line to $\varepsilon_{zz} = 0\%$.

3 Mesoscale analysis of the grain transport mechanism

If the grain detachment mechanism is closely linked to the stress transmission through the solid phase of granular materials, the grain transport mechanism is fundamentally linked to the properties of the dual phase, namely the pore space. In the rest of this study, potential electrostatic interactions between particles are disregarded and it is assumed that the ability of a grain to be transported is purely based on geometrical considerations. As a result, the complex description of the pore space can be reduced to the definition of a graph composed of pores (the nodes of the graph) and constrictions (the edges of the graph). The definition of this graph is derived from a tessellation of the granular assembly as in [4] and [6], and Figure 3 provides an illustration of this type of graph for simple grains assemblies.

The pores are defined following the level 0 analysis introduced in [4]. Their positions are defined at the center of each tetrahedron of a regular Delaunay triangulation and their radii as the radius of the largest interior sphere in the associated tetrahedra (Figure 3.a). The constrictions are modeled as cylinders joining two adjacent pores and their radii are defined as the radius of the largest interior circle on the common face of the two tetrahedra defining the constriction (Figure 3.b).

In order to assess the possibility for the grains composing a granular material to be transported, it is interesting to compare the grain radius distribution to the pore and constriction radius distributions characterizing the void space. In Figure 4 the probability densities for a fictive particle of a given radius to find a pore or a constriction large enough to fit in are plotted together with the probability densities corresponding to the radius distribution of the chained and non-chained grains identified in the previous section. These probability densities are given at the beginning and at the end of the triaxial compression introduced in Section 1.

The comparison between the constriction probability density and the non-chained grain probability density in Figure 4 highlights that a large number of non-chained grains are small enough to be transported through the pore network as 33 to 34 % of these grains have a radius smaller than the mean constriction radius plus one standard deviation. On the contrary, very few chained grains are small enough to fit in the pores and constrictions.

While observing the strain evolution of the constriction probability density, the contractive/dilative behavior typical of dense granular materials is recovered. Indeed, the probability densities are shifted toward larger radius values, which is related to an overall increase of the pore space volume.

Even though many particles are identified in Figure 4 as potentially transportable by analyzing the statistical properties of the pore network, the definition of a mesoscale associated with the grain transport mechanism requires knowing the spatial distribution of pores and constrictions together with the fluid flow direction. If the definition of the pore network proposed in this section provide the spatial distribution of the pores and constrictions under the form of a non-oriented mathematical graph, there is a need to define a propagation criterion on this graph to incorporate the forcing imposed by the internal flow with respect to grain transport. For a given flow direction (taken along the direction $\boldsymbol{e}_x$ in Figure 1 for the rest of this study), the definition of such propagation criterion is achieved thanks to the combined used of the DEM-PFV model implemented in YADE software [7]:

- First, the DEM-PFV scheme is used to generate a pressure map in the pore network under a fluid flow imposed by a small pressure drop between the sample boundaries in the x direction;

- Then, based on the Hagen-Poiseuille flow velocity profile for a circular tube and the expression of the drag force of a uniform flow acting on a sphere for low Reynolds numbers, a flow intensity indicator is defined in each constriction as $\frac{\Delta p}{\ell} \times R^2$ with ℓ being the length of the constriction, Δp the pressure drop between the two adjoining pores and R the constriction radius;

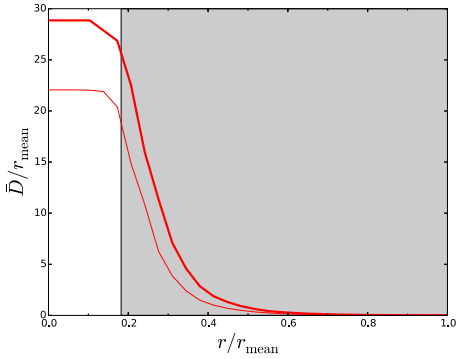

Figure 5. Mean travel distance for different radius thresholds. The thick line corresponds to $\varepsilon_{zz} = 20\%$, while the thin line to $\varepsilon_{zz} = 0\%$. The grey domain in the background corresponds to the radius values for the grains composing the sample.

- Finally, a transport path is defined for a given particle of radius r and for a given starting pore as the path of maximum flow intensity on the restriction of the pore network to pores and constrictions of radii larger than r.

For a given radius r, a mean travel distance $\bar{D}(r)$ is then computed from statistical averaging of the length of all the existing transport path. This quantity stands for a measure of the typical length associated with grain transport mechanism. In Figure 5, $\bar{D}(r)$ is plotted for the two same sample configurations used in Figure 4.

For these two configurations, the mean travel distance decreases from $22 - 29\, r_{\mathrm{mean}}$ to zero. If no transport is possible for particles larger than roughly $0.5\, r_{\mathrm{mean}}$ the smallest particles of the considered sample have good chances to be transported over large distances going up to $25\, r_{\mathrm{mean}}$ representing roughly half of the total length of the sample. The comparison between these typical length scales associated with grain transport with the ones associated with grain detachment obtained in the previous section highlights a separation of scale between the two mechanisms provided that the detached grains are found among the smallest particles of the sample considered.

4 Conclusion and outlooks

In this paper, specific micromechanical tools are developed to investigate the susceptibility of a polydisperse assembly of spherical particles to grain detachment and grain transport. By simultaneously considering the size distributions of the non-chained particles and the constrictions of the pore network, the ability of a fluid flow to modify the microstructure of the samples is analyzed with respect to the fraction of both potentially detachable and transportable particles which represents approximately 25% of the non-chained ones. During a drained triaxial test, it is found that the microstructure of the dense sample considered evolves towards a configuration more favorable to observe the detachment and the transport of grains within the sample volume. Indeed, as the axial stress increases during the triaxial test, the number of chained particles tends to decrease which results in larger groups of potentially detachable particles. In the meantime, as our sample exhibit a dilative behavior, the pores and constrictions get larger which results in an increase of the travel distances accessible to detached particles. As a result, for a same grading curve, our micromechanical analysis predicts a higher suffusion susceptibility of our sample at the critical state than in the initial dense configuration at the beginning of the triaxial testing.

By carefully considering the spatial distribution of particles participating in stress transmission and the spatial distribution of constrictions enabling particle transport within the pore space, two mesoscales are introduced to study the grain detachment and the grain transport processes from a micromechanical point of view. It was shown that the typical length scale associated with grain transport can be up to ten times larger than that associated with grain detachment. As a result, a scale separation should exist between these two processes provided that the detached grains are found among the smallest particles of the sample considered.

Eventually, as the order of magnitude of the introduced length scales is still relatively small compare to the total length of the considered sample ($48 r_{\mathrm{mean}}$), full 3D modeling of the suffusion process is accessible and can be used to confirm this scale separation as well as to explore the local conditions leading to the occurrence of grain detachment and transport. This would pave the way for the definition of a homogenized law for suffusion thanks to the use of representative elementary volumes sufficiently big with respect to these two elementary mechanisms.

References

[1] S. Bonelli, *Erosion of geomaterials* (John Wiley & Sons, 2012)
[2] J.F. Peters, M. Muthuswamy, J. Wibowo, A. Tordesillas, Physical review E **72**, 041307 (2005)
[3] T. Kanit, S. Forest, I. Galliet, V. Mounoury, D. Jeulin, International Journal of solids and structures **40**, 3647 (2003)
[4] N. Reboul, E. Vincens, B. Cambou, Granular Matter **10**, 457 (2008)
[5] P.A. Cundall, O.D. Strack, Geotechnique **29**, 47 (1979)
[6] E. Vincens, K.J. Witt, U. Homberg, Acta Geotechnica **10**, 291 (2015)
[7] B. Chareyre, A. Cortis, E. Catalano, E. Barthélemy, Transport in porous media **94**, 595 (2012)